

Assembly of Two Mesoporous Anionic Metal–Organic Frameworks for Fluorescent Sensing of Metal Ions and Organic Dyes Separation

Yu-Hui Luo,* A-Di Xie, Ming-Gai Hu, Ji Wu, Dong-En Zhang, and Ya-Qian Lan*

Cite This: *Inorg. Chem.* 2021, 60, 167–174

Read Online

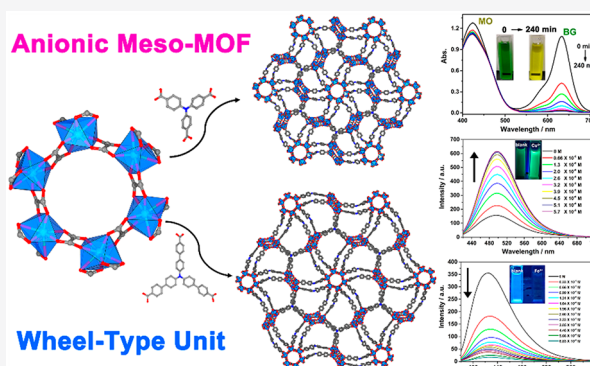
ACCESS |

Metrics & More

Article Recommendations

Supporting Information

ABSTRACT: Anionic metal–organic frameworks (MOFs) have attracted increasing attention due to the enhanced electrostatic interactions between their anionic frameworks and counter-ionic guests. Owing to these special host–guest interactions, anionic MOFs are beginning to have a large impact in the field of absorption and separation of ionic molecules and selective sensing of metal ions. Herein, two mesoporous anionic metal–organic frameworks, namely, $[(\text{CH}_3)_2\text{NH}_2]_6[\text{In}_6(\text{OX})_6(\text{TCA})_4]\cdot\text{solvents}$ (**JOU-11**) and $[(\text{CH}_3)_2\text{NH}_2]_6[\text{In}_6(\text{OX})_6(\text{TCPA})_4]\cdot\text{solvents}$ (**JOU-12**) (H_3TCA = tricarboxytriphenylamine; H_3TCPA = tris((4-carboxyl)phenylduryl)amine; OX = oxalate), have been synthesized by using wheel-type $[\text{In}_6(\text{OX})_6(\text{COO})_{12}]^{6-}$ as building blocks. Structural analyses show that **JOU-11** and **JOU-12** show isorecticular three-dimensional frameworks with **pyr** topology. Due to their anionic frameworks and tunable pore window sizes, both compounds can be exploited for absorbing and separating cationic organic dyes. In addition, **JOU-11** can be developed as a fluorescence “turn-off” sensor for selectively sensing Fe^{3+} , whereas **JOU-12** can be used for fluorescence “turn-on” sensing of Cu^{2+} and Co^{2+} ions.



INTRODUCTION

Anionic metal–organic frameworks (MOFs) represent a subclass of the MOF family and are attracting increasing attention over the past decades.^{1–5} Electrostatic force between the anionic framework and cationic guests can enhance host–guest interactions, resulting in many promising applications, such as absorption, sensing, and biotechnology.^{6–8} On the basis of their structural features, anionic frameworks can also be applied to selective capturing and separating ionic small molecules, such as organic pollutants, pharmaceutical molecules, and so on. Rosi et al. have developed anionic bio-MOF-1 as a host to encapsulate and sensitize lanthanide cations.⁹ Su and colleagues have reported the synthesis of anionic framework for organic dyes separation.¹⁰ Recently, many other research groups have put their efforts on designing anionic MOFs especially for organic dyes absorption and separation.^{11–13} It has been shown that the pore window size of MOFs is an important factor for this purpose.^{14,15} In particular, MOFs with pore window sizes larger than 2 nm are desirable. However, examples of anionic MOFs with pore windows of this size are sparse in the literature.¹⁶ Thus, it remains a challenge to prepare new mesoporous anionic MOFs for absorbing and separating organic dyes.

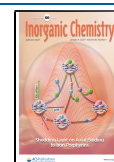
On the other hand, metal ions are widespread in nature and play an important role in the environment and living body.^{17–19} In the human body, the concentration of metal ions within a certain range is very important for life and health,

while a lower or higher concentration of metal ions will cause diseases, such as glycuris, diarrhea, and Alzheimer’s disease.²⁰ Thus, it is particularly important to detect selective metal ions. In past decades, MOFs have shown promising applications in fast responsive and selective trace metal ion detection.^{21–25} Some MOFs with light-emitting ligands have been developed as fluorescent probes for detecting metal ions, including Cr^{3+} , Fe^{3+} , Cu^{2+} , etc.^{26–28} In this respect, a fluorescence “turn-on” MOF is desired because it exhibits fluorescence-enhanced response under test conditions. However, most of the reported fluorescent MOF probes are based on “turn-off” detection. In particular, fluorescence “turn-on” MOFs for Cu^{2+} and Co^{2+} sensing are quite rarely reported.^{29,30} Up to now, many efforts have been devoted to develop MOFs as fluorescence “turn-on” sensors for trace metal ions detection.²⁹

Recently, the second building unit (SBU) approach is wildly used for the design and construction of MOFs.^{31,32} It has been proved that the rational selection of SBUs can not only develop ionicity in MOFs but also prepare MOFs with large and

Received: September 16, 2020

Published: December 16, 2020



tunable pores. For instance, Bu et al. have reported the design and synthesis of cationic MOFs by investigating cationic metal clusters $[\text{M}_3\text{O}(\text{COO})_6]^+$ ($\text{M} = \text{In}^{3+}$, Fe^{3+} , Al^{3+} , ...).^{33–35} In contrast, anionic MOFs with various networks can be constructed by using anion building units such as $[\text{In}(\text{COO})_4]^-$.^{36–38} On the basis of the above-mentioned considerations, we aimed to prepare mesoporous fluorescent anionic MOFs with tunable pore window sizes by using suitable anionic SBUs and light-emitting ligands. The wheel-type six-membered indium-oxalate ring, formulated as $[\text{In}_6(\text{OX})_6(\text{COOH})_{12}]^{6-}$ ($\text{OX} = \text{oxalate}$), was investigated for its negative charge and potential high coordination numbers. Triphenylamine-based carboxylic acids were selected as ligands for their various coordination modes and good luminescent properties. Herein, two newly designed anionic MOFs, namely, $[(\text{CH}_3)_2\text{NH}_2]_6[\text{In}_6(\text{OX})_6(\text{TCA})_4] \cdot \text{solvents}$ (**JOU-11**) and $[(\text{CH}_3)_2\text{NH}_2]_6[\text{In}_6(\text{OX})_6(\text{TCPA})_4] \cdot \text{solvents}$ (**JOU-12**) ($\text{H}_3\text{TCA} = \text{tricarboxytriphenylamine}$; $\text{H}_3\text{TCPA} = \text{tris}((4\text{-carboxyl})\text{phenylduryl})\text{amine}$), are synthesized by tuning the length of organic ligands. Structural studies show that **JOU-11** and **JOU-12** represent isoreticular three-dimensional (3D) mesoporous anionic frameworks with tailored pore sizes. Moreover, the two compounds demonstrate various applications in organic dyes absorption and separation, fluorescence “turn-on” sensing of Cu^{2+} and Co^{2+} , and selective “turn-off” sensing of Fe^{3+} by virtue of their anionic frameworks, extensible pore window sizes, and good fluorescence properties.

RESULTS AND DISCUSSION

Crystal Structure of MOFs. Compounds **JOU-11** and **JOU-12** show isoreticular frameworks and both crystallize in the cubic space group $Pa\bar{3}$. Both compounds display 3D frameworks based on $[\text{In}_6(\text{OX})_6(\text{COO})_{12}]^{6-}$ building blocks and tricarboxylic ligands (Figure 1a–c). The asymmetric units of them contain one crystallographically independent In^{3+} ion, one oxalate, and two one-third $\text{TCA}^{3-}/\text{TCPA}^{3-}$ ligands. In1 coordinates to eight oxygen atoms from two oxalates and two carboxylate groups (Figure S1 (Supporting Information)). In–O bond lengths are in the range of 2.108(12)–2.574(15) Å for **JOU-11** and in the range of 2.173(14)–2.434(15) Å for **JOU-12**. As shown in Figure 1c, six In^{3+} ions are linked by six oxalates to form a wheel-type six-membered indium-oxalate ring with an internal diameter of about 8.6 Å. Thereafter, the wheel-type indium-oxalate rings are connected by tricarboxylic ligands to generate a 3D non-interpenetrated negatively charged framework. It is found that the frameworks of **JOU-11** and **JOU-12** feature two types of cages, and the sizes of cages increase as the lengths of organic ligands increase (Figure 1d–g). The diameter sizes of small and large cages of **JOU-11** are about 16.1 and 26.6 Å, whereas those of **JOU-12** are about 21.9 and 37.1 Å, respectively. Take **JOU-12** for example, each large cage is surrounded by six small cages, and each small cage is surrounded by three large cages and one other small cage (Figure 2a,b). These cages are cross-linked within the structure to form 3D channels (Figure 2c). PLATON calculation indicates very high porosities of 73.5% and 84.0% in **JOU-11** and **JOU-12**, respectively.³⁹ Negative charges of the frameworks are balanced by protonated dimethylamine derived from the decomposition of solvent DMF. These cationic $[(\text{CH}_3)_2\text{NH}_2]^+$ ions are distributed disorderedly in the void spaces of MOFs. Topologically, each group of parallel adjacent tricarboxylic ligands connected with three indium-oxalate rings

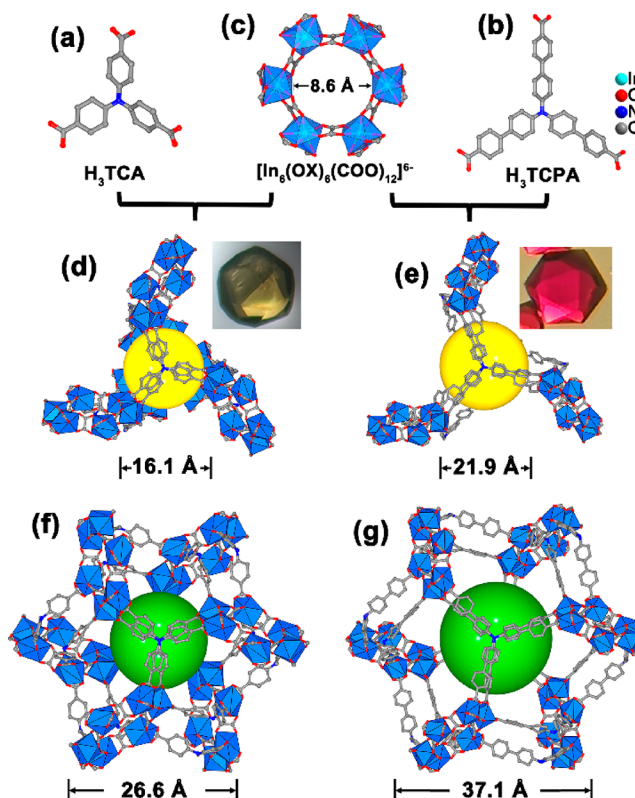


Figure 1. (a)–(c) represent the structure of H_3TCA , wheel-type $[\text{In}_6(\text{OX})_6(\text{COO})_{12}]^{6-}$ unit, and H_3TCPA , respectively. (d) and (e) represent the small cage of **JOU-11** and **JOU-12**, respectively. Inset photographs in (d) and (e) exhibit the crystal of **JOU-11** and **JOU-12**, respectively. (f) and (g) show the large cage of **JOU-11** and **JOU-12**, respectively.

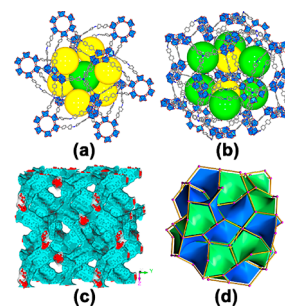


Figure 2. (a) Each large cage of **JOU-12** (shown as green ball) is surrounded by six small cages (shown as yellow ball). (b) Each small cage of **JOU-12** is surrounded by three large cages and one other small cage. (c) View of the 3D channels of **JOU-12**. (d) Tiling of **JOU-12**.

can be simplified as a 3-connected node (Figure S2). Each indium-oxalate ring coordinated by six groups of parallel tricarboxylic ligands can be considered as a 6-connected node. Thus, the network of the title compounds can be reduced to a (3,6)-connected *pyr* topology (Figure 2d). Both compounds are further characterized by powder X-ray diffraction (PXRD) (Figure S3), thermogravimetric analysis (TGA) (Figure S4), and Fourier transform infrared spectroscopy (FT-IR).

Organic Dyes Absorption and Separation. Due to their porous and charged structural features, **JOU-11** and **JOU-12** were applied for selective absorbing and separating organic dyes. Five widely used organic dyes were chosen for studies

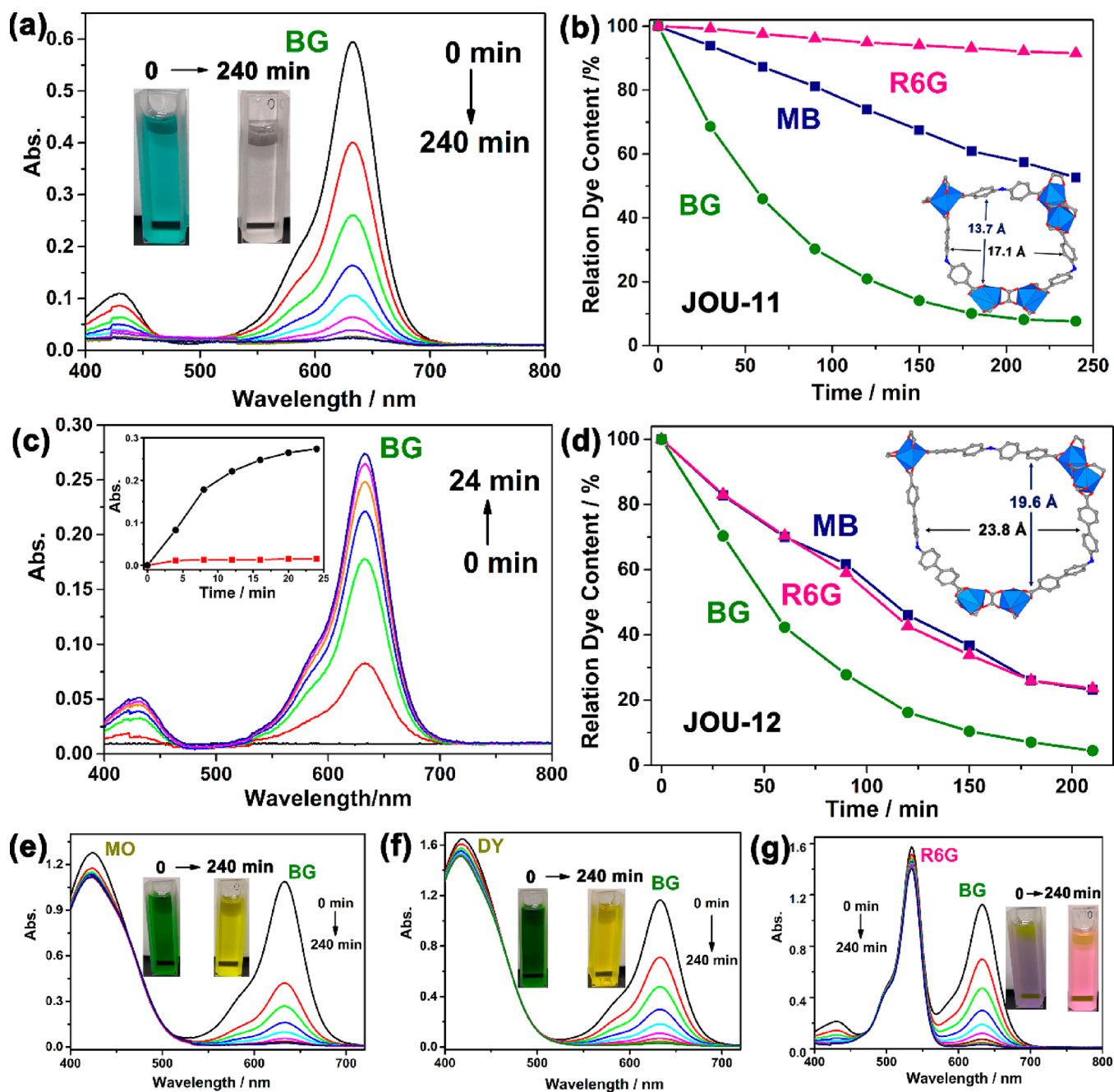


Figure 3. (a) BG is absorbed by JOU-11 gradually. Inset photos: Color of BG solution changes from green to colorless during sorption process. (b) Absorption kinetics of JOU-11. The inset graph shows the pore window size of JOU-11. (c) BG released from BG@JOU-11 in the presence of Na⁺ ions. The inset graph shows the release kinetics curves of BG@JOU-11 in a NaCl solution (black) and pure DMF (red), respectively. (d) Absorption kinetics of JOU-12. The inset graph shows the pore window size of JOU-12. Panels (e)–(g) show the UV–vis absorption spectra of BG/MO, BG/DY, and BG/R6G solution, respectively. Inset photos: After 4 h sorption, the color of the mixed dyes' solution changes to the color of residual dye.

(Figure S5), including cationic dyes (brilliant green (BG), methylene blue (MB), and rhodamine 6G (R6G)), a neutral dye (dimethyl yellow (DY)), and an anionic dye (methyl orange (MO)). In this part, the absorption behaviors of JOU-11 were first discussed in detail, and then these behaviors were compared with those of JOU-12. First, the freshly synthesized crystals (30 mg) of JOU-11 were immersed in different dyes DMF solutions. After soaking for different periods of time, the absorption capacities of dyes are determined by the absorption intensities of the corresponding dyes. As expected, JOU-11 can absorb all three selected cationic dyes. As shown in Figures 3a

and S6, cationic dyes were quickly absorbed by JOU-11, leading to a color change throughout the crystals (Figure S7). In contrast, small neutral dye DY can only be absorbed slowly, which may be due to the lack of host–guest electrostatic interactions (Figure S8). For the anionic dye MO, only negligible absorption was obtained with JOU-11. This is consistent with our expectation that the anionic framework does not absorb anionic dyes. The absorption properties of the title compounds were evaluated with MB as a representative. The MB loading amounts of JOU-11 and JOU-12 were calculated to be 354.8 and 148.6 mg g^{−1}, respectively. These

absorption performances are compared with those of other reported MOFs (Table S4). The absorption kinetics of JOU-11 for different cationic molecules are shown in Figure 3b. It can be found that the absorption rates of different cationic organic dyes were different. This may be due to the size effect and different host–guest interactions. Obviously, as BG has a much smaller molecular volume than R6G, the absorption rate of BG is higher. In contrast, although the molecular size of MB is smaller than BG, a lower absorption rate of MB was obtained. This may be due to the different host–guest interactions, such as the hydrogen-bonding interactions between MB and the framework of JOU-11. On the other hand, dyes absorbed in JOU-11 can be released by soaking the MOF loaded with dyes in a saturated NaCl solution of DMF (Figures 3c and S6). As shown in Figure 3c, when the MOF loaded with BG was put into a NaCl solution, the absorption intensities of BG gradually increased with time, indicating the release of BG molecules. However, the dye-loaded MOF hardly released dye molecules in pure DMF. These results indicate that BG is released via an ion-exchange process with the assistance of Na^+ as a trigger.^{36,40}

The different absorption behaviors of JOU-11 for different organic dyes can be developed for dye separation. As shown in Figure 3e, when crystals of JOU-11 were soaked in a mixed solution of MO and BG (1:1 in mole ratio), the color of the mixed solution gradually changed from green to yellow. This is attributed to that BG is selectively absorbed, which is also proved by the UV–vis absorption spectra (Figure 3e). A similar selectivity can also be found in a mixed solution of DY and BG (Figure 3f). It is interesting that cationic dyes with different sizes can also be separated. For example, when crystals of JOU-11 were put into a mixed solution of R6G and BG in a 1:1 mole ratio, BG was preferentially absorbed. This is because the molecular volume of BG is much smaller than that of R6G. These results show that JOU-11 is more inclined to absorb cationic dyes. The absorption process is achieved through ion exchange between $[(\text{CH}_3)_2\text{NH}_2]^+$ in the channels of JOU-11 and cationic dye molecules. These absorbed cationic dyes can also be released in a NaCl solution.

For JOU-12, it shows similar dye absorption and separation behaviors to JOU-11 as it has a similar structure (Figure S9). On the other hand, as the pore window size of JOU-12 ($19.6 \text{ \AA} \times 23.8 \text{ \AA}$) is much larger than that of JOU-11 ($13.7 \text{ \AA} \times 17.1 \text{ \AA}$), it shows a much faster R6G absorption rate than JOU-11 (Figure 3d). These results further prove that the size effect is important for organic dyes absorption. As an example, the PXRD patterns of compounds JOU-11 and JOU-12 show little change after releasing BG dyes, indicating their stability for organic dye absorbing and releasing (Figure S10).

Fluorescence “Turn-On” Sensing of Cu^{2+} and Co^{2+} Ions. Solid state fluorescence spectra of JOU-11 and JOU-12 show emission bands peaking at 423 and 492 nm, respectively (Figures S11 and S12). These emission bands may be originated from the intra-ligand charge transfer of corresponding tricarboxylic ligands. Compared to the corresponding free ligands, the blue shift of the emission peaks of JOU-11 and JOU-12 may arise from the deprotonation and coordination effect.^{41–43} On the basis of these fluorescent characteristics, we developed JOU-11 and JOU-12 as potential metal ions sensors. First, the crystals of JOU-11 and JOU-12 were finely grounded into powder and then dispersed into DMF solutions in a concentration of 1 mg mL^{-1} , respectively. These mixtures were ultrasonically treated for 1 h and then aged overnight.

Fifteen kinds of metal ions are selected for sensing studies, including K^+ , Na^+ , Cu^{2+} , Co^{2+} , Cr^{3+} , Mg^{2+} , Mn^{2+} , Ca^{2+} , Zn^{2+} , Ba^{2+} , Cd^{2+} , Pb^{2+} , Ni^{2+} , Fe^{3+} , and Al^{3+} . Emission peaks of JOU-11 and JOU-12 in DMF solution are similar to the corresponding solid fluorescence. As shown in Figures 4a,

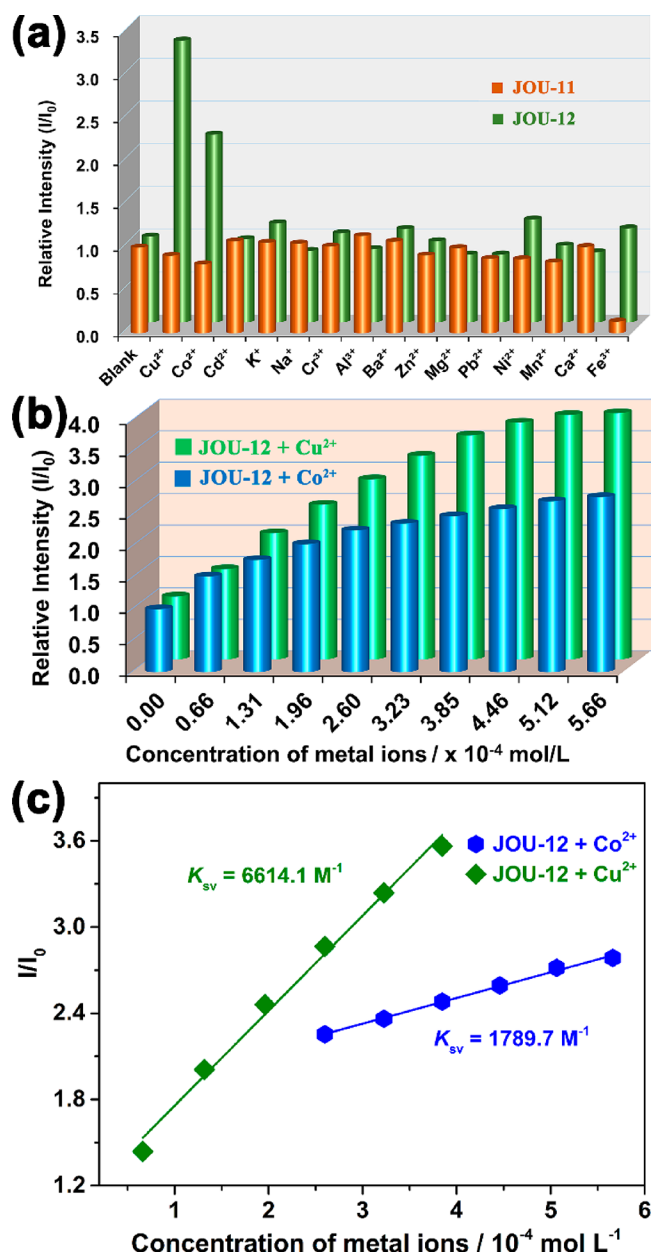


Figure 4. (a) Relative emission peak intensity of JOU-11 and JOU-12 in the presence of different metal ions. (b) Relative fluorescent peak intensities of JOU-12/ Cu^{2+} and JOU-12/ Co^{2+} . (c) Stern–Volmer plots of JOU-12.

S13 and S14, when different metal ions were added to the aged MOF dispersion with the same concentration, the luminescent intensity peaked at 495 nm for JOU-12 was significantly enhanced when Cu^{2+} or Co^{2+} was added. These results reveal that JOU-12 can be used as a fluorescent probe for Cu^{2+} and Co^{2+} ions sensing. We further studied the fluorescence enhancement effect of JOU-12 as a function of $\text{Cu}^{2+}/\text{Co}^{2+}$ concentration (Figures 4b and S15). It can be found that the emission peak intensities of JOU-12 are highly responsive to

the concentration of Cu^{2+} or Co^{2+} ions. For the Cu^{2+} ion, the emission peak of JOU-12 increased gradually as Cu^{2+} concentration increased within the range of $0\text{--}5.66 \times 10^{-4} \text{ mol L}^{-1}$. For Co^{2+} , the emission peak of JOU-12 increased as Co^{2+} concentration increased over the range of $0\text{--}1.1 \times 10^{-3} \text{ mol L}^{-1}$. The fluorescent peak intensity of JOU-12 vs the concentration of metal ions can be curve-fitted into $I_0/I = 1.10 + 6614.1 [\text{Cu}^{2+}]$ ($R^2 = 0.990$) for Cu^{2+} ion and $I_0/I = 1.79 + 1789.7 [\text{Co}^{2+}]$ ($R^2 = 0.995$) for Co^{2+} ion (Figure 4c). These results are consistent with the Stern–Volmer equation: $I_0/I = 1 + K_{\text{SV}}[M]$, where I_0 represents the initial fluorescence peak intensity of the JOU-12 dispersion, I indicates the fluorescence peak intensity of the JOU-12 dispersion in the presence of metal ions, $[M]$ indicates the molar concentration of metal ion, and K_{SV} is the Stern–Volmer constant.⁴⁴ The limits of detection (LODs) for Cu^{2+} and Co^{2+} were, respectively, determined to be 1.82×10^{-5} and $6.74 \times 10^{-5} \text{ mol L}^{-1}$ by using the $\text{LOD} = 3s/K_{\text{SV}}$ equation, where s represents the standard deviation of the blank. These results reveal that JOU-12 can act as a fluorescence “turn-on” probe for Cu^{2+} and Co^{2+} ions sensing. To explore the mechanism of fluorescence enhancement, further tests have been investigated. First, the dispersions of pure MOF, MOF/ Cu^{2+} , and MOF/ Co^{2+} were, respectively, centrifuged by using a high-speed centrifuge, resulting in three parts of supernatant, which were analyzed by fluorescence and UV–vis spectra (Figure S16). It is found that supernatants obtained from MOF/ Cu^{2+} and MOF/ Co^{2+} also exhibit strong fluorescence intensities, whereas the supernatant obtained from pure MOF shows negligible fluorescence intensity. These results further confirm that the decomposition of the MOF occurs with $\text{Cu}^{2+}/\text{Co}^{2+}$ as a trigger. Therefore, the fluorescence enhancement of JOU-12 is most likely attributed to the dissociation of the framework in the aid of Cu^{2+} or Co^{2+} ion.

Fluorescence “Turn-Off” Sensing of Fe^{3+} Ions. The fluorescent intensity peaked at 424 nm for JOU-11 was significantly reduced when Fe^{3+} was added (Figure 4a). This result indicates that JOU-11 can be developed as a fluorescent probe for sensing of Fe^{3+} . The quenching effect of JOU-11 as a function of Fe^{3+} concentration was also studied (Figure S18). The emission peak of JOU-11 reduced gradually as the concentration of Fe^{3+} increased. The fluorescent peak intensity of JOU-11 vs the concentration of Fe^{3+} can be curve-fitted into $I_0/I = 1.02 + 26626.5 [\text{Fe}^{3+}]$ ($R^2 = 0.998$) (Figure 5). This result is also consistent with the Stern–Volmer equation: $I_0/I = 1 + K_{\text{SV}}[M]$.⁴⁴ The LOD of JOU-11 was calculated to be $4.53 \times 10^{-6} \text{ mol L}^{-1}$ for Fe^{3+} . As shown in Table S5, K_{SV} and LOD values for JOU-11 toward Fe^{3+} sensing are comparable to those of other reported MOF-based materials. The selectivity of JOU-11 toward Fe^{3+} sensing was also verified by comparative experiments. As shown in Figure S19, the emission intensity of JOU-11 did not change significantly after adding 14 kinds of metal ions, including K^+ , Na^+ , Cu^{2+} , Co^{2+} , Cr^{3+} , Mg^{2+} , Mn^{2+} , Ca^{2+} , Zn^{2+} , Ba^{2+} , Cd^{2+} , Pb^{2+} , Ni^{2+} , and Al^{3+} . However, the emission peak of JOU-11 reduced significantly when Fe^{3+} ions are added, indicating high selectivity of JOU-11 toward Fe^{3+} sensing. These results reveal that JOU-11 can

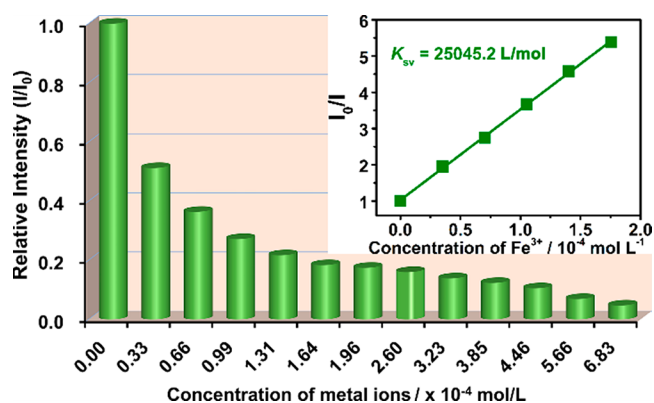


Figure 5. Relative emission peak intensity of JOU-11 in the presence of different concentrations of Fe^{3+} . Inset: Stern–Volmer plot of JOU-11.

act as a fluorescence “turn-off” probe for selective detection of Fe^{3+} ions in complex systems. In addition, both JOU-11 and JOU-12 can be stable in a mixed solution of DMF/water (V/V, 2:1) over 24 h (Figure S20). As shown in Figure S21, as the concentration of water increased, the position and intensity of the emission band mainly remain unchanged. On the basis of these results, these compounds may be developed as a fluorescence probe for sensing metal ions in wastewater in the future.

In order to explore the quenching mechanism, the following experiments were carried out. First, crystals of JOU-11 were immersed in the Fe^{3+} DMF solution for 24 h. Then, the crystals were filtered out for XRD analysis, and the filtrate was also collected for UV–vis analysis. It is shown that the PXRD pattern of JOU-11 after immersing in Fe^{3+} solution matches well with the simulated one, and the UV–vis absorption spectrum of the filtrate only shows the characteristic absorption peak of Fe^{3+} (Figure S22). These results reveal that JOU-11 is stable during sensing tests. Thus, structural decomposition must not be the reason for fluorescence quenching. Then, the UV–vis absorption spectra of JOU-11 and JOU-11/ Fe^{3+} dispersions were recorded. It is found that a new absorption band centered at about 331 nm appears and the peak intensity enhanced gradually with Fe^{3+} concentration increases (Figure S23), indicating electrostatic interactions occur between the Fe^{3+} ions and JOU-11. These electrostatic interactions may cause fluorescence quenching through a photo-induced electron/charge transfer (PET) process.^{46,47} In addition, as the absorption band of Fe^{3+} in DMF solution covers the emission band of JOU-11, fluorescence resonance energy transfer (FRET) may also occur (Figure S24).^{47–49} Therefore, the decrease of the peak intensity of JOU-11 in the presence of Fe^{3+} may be due to the combination of PET and FRET effects.

CONCLUSIONS

In summary, two isorecticular mesoporous anionic MOFs with a (3,6)-connected pyr topology were prepared based on a wheel-type $[\text{In}_6(\text{OX})_6(\text{COO})_{12}]^{6-}$ building block and length-extendable tricarboxylic ligands. Due to their charged frameworks and tunable pore window sizes, JOU-11 and JOU-12 can selectively absorb and release organic dyes through ion-exchange processes. Furthermore, the singular dye absorption behaviors of JOU-11 are exploited not only to separate dye molecules with different charges but also to separate cationic

dyes with different molecular sizes. In addition, owing to the successful introduction of fluorescent ligands, both J_{OU}-11 and J_{OU}-12 have been explored as fluorescent probes for metal ions sensing. Fascinatingly, J_{OU}-11 can act as a fluorescence “turn-off” sensor for selectively sensing Fe³⁺ ion, whereas J_{OU}-12 can act as an unusual fluorescence “turn-on” probe for Cu²⁺ and Co²⁺ ions detection. This work provides valuable clues for the construction of multifunctional MOFs, which may probably be used in the field of organic dye absorption and separation and fluorescent metal ions sensing. By employing different tailorable anionic building blocks, the synthesis and exploration of novel anionic MOFs are currently in progress.

EXPERIMENTAL SECTION

Synthesis of J_{OU}-11. A mixture of In(NO₃)₃·4.5H₂O (0.05 mmol, 15 mg), H₃TCA (0.02 mmol, 7.5 mg), OX (0.02 mmol, 2 mg), DMF (1.2 mL), MeCN (0.5 mL), and HNO₃ (65%, 40 μL) was stirred under air for 2 h and was then transferred into a 10 mL glass bottle. After being heated at 85 °C for 72 h, yellow polyhedral crystals were obtained in a yield of 35% (based on H₃TCA). CCDC number for J_{OU}-11 is 2019926. IR (KBr, cm⁻¹): ν = 3442 (s), 3060 (m), 2977 (m), 2799 (m), 1660 (s), 1596 (s), 1531 (m), 1407 (s), 1382 (s), 1315 (s), 1270 (m), 1176 (m), 1108 (m), 1024 (m), 875 (w), 784 (m), 678 (s), 532 (s).

Synthesis of J_{OU}-12. The synthesis process of J_{OU}-12 is similar to that of J_{OU}-11 except that H₃TCA was replaced with H₃TCPA (0.02 mmol, 12 mg). Red polyhedral crystals were collected in a yield of about 30% (based on H₃TCPA). CCDC number for J_{OU}-12 is 2019927. IR (KBr, cm⁻¹): ν = 3446 (s), 3043 (m), 2964 (m), 2796 (m), 1654 (s), 1604 (s), 1525 (s), 1488 (s), 1421 (s), 1384 (s), 1284 (m), 1187 (m), 1099 (m), 1020 (m), 877 (m), 836 (m), 786 (s), 725 (m), 659 (m), 489 (m).

ASSOCIATED CONTENT

Supporting Information

The Supporting Information is available free of charge at <https://pubs.acs.org/doi/10.1021/acs.inorgchem.0c02760>.

Instrumentation, single-crystal X-ray diffraction and powder X-ray diffraction data, figures of MOFs, dyes' absorption, and MOFs' photoluminescence spectra (PDF)

Accession Codes

CCDC 2019926 and 2019927 contain the supplementary crystallographic data for this paper. These data can be obtained free of charge via www.ccdc.cam.ac.uk/data_request/cif, or by emailing data_request@ccdc.cam.ac.uk, or by contacting The Cambridge Crystallographic Data Centre, 12 Union Road, Cambridge CB2 1EZ, UK; fax: +44 1223 336033.

AUTHOR INFORMATION

Corresponding Authors

Yu-Hui Luo — School of Environmental and Chemical Engineering, Jiangsu Ocean University, Lianyungang 222000, Jiangsu Province, People's Republic of China; Email: luoyh@jou.edu.cn

Ya-Qian Lan — School of Chemistry and Materials Science, Nanjing Normal University, Nanjing 210023, Jiangsu Province, People's Republic of China; orcid.org/0000-0002-2140-7980; Email: yqlan@njnu.edu.cn

Authors

A-Di Xie — School of Environmental and Chemical Engineering, Jiangsu Ocean University, Lianyungang 222000, Jiangsu Province, People's Republic of China

Ming-Gai Hu — School of Environmental and Chemical Engineering, Jiangsu Ocean University, Lianyungang 222000, Jiangsu Province, People's Republic of China

Ji Wu — School of Environmental and Chemical Engineering, Jiangsu Ocean University, Lianyungang 222000, Jiangsu Province, People's Republic of China

Dong-En Zhang — School of Environmental and Chemical Engineering, Jiangsu Ocean University, Lianyungang 222000, Jiangsu Province, People's Republic of China

Complete contact information is available at:

<https://pubs.acs.org/10.1021/acs.inorgchem.0c02760>

Notes

The authors declare no competing financial interest.

ACKNOWLEDGMENTS

This work was financially supported by the Six Talents Peak Project of Jiangsu Province (XCL-009); the Foundation of Jiangsu Key Laboratory of Function Control Technology for Advanced Materials (AM201902); the Priority Academic Program Development of Jiangsu Higher Education Institutions (PAPD); and the Graduate Student Training Innovation Project of Jiangsu Province (KYCX19-2261).

REFERENCES

- (1) Karmakar, A.; Desai, A. V.; Ghosh, S. K. Ionic Metal-Organic Frameworks (iMOFs): Design Principles and Applications. *Coord. Chem. Rev.* **2016**, *307*, 313–341.
- (2) Li, P.; Vermeulen, N. A.; Gong, X.; Malliakas, C. D.; Stoddart, J. F.; Hupp, J. T.; Farha, O. K. Design and Synthesis of a Water-Stable Anionic Uranium-Based Metal-Organic Framework (MOF) with Ultra Large Pores. *Angew. Chem., Int. Ed.* **2016**, *55*, 10358–10362.
- (3) Gosselin, E. J.; Decker, G. E.; Antonio, A. M.; Lorz, G. R.; Yap, G. P. A.; Bloch, E. D. A Charged Coordination Cage-Based Porous Salt. *J. Am. Chem. Soc.* **2020**, *142*, 9594–9598.
- (4) Yang, S.; Lin, X.; Blake, A. J.; Walker, G. S.; Hubberstey, P.; Champness, N. R.; Schröder, M. Cation-Induced Kinetic Trapping and Enhanced Hydrogen Adsorption in a Modulated Anionic Metal-Organic Framework. *Nat. Chem.* **2009**, *1*, 487–493.
- (5) Cui, Y.; Song, T.; Yu, J.; Yang, Y.; Wang, Z.; Qian, G. Dye Encapsulated Metal-Organic Framework for Warm-White LED with High Color-Rendering Index. *Adv. Funct. Mater.* **2015**, *25*, 4796–4802.
- (6) Zeng, Q.; Wang, L.; Huang, Y.; Zheng, S. L.; He, Y.; He, J.; Liao, W. M.; Xu, G.; Zeller, M.; Xu, Z. An Air-Stable Anionic Two-Dimensional Semiconducting Metal-Thiolate Network and Its Exfoliation into Ultrathin Few-Layer Nanosheets. *Chem. Commun.* **2020**, *56*, 3645–3648.
- (7) Qin, J. S.; Zhang, S. R.; Du, D. Y.; Shen, P.; Bao, S. J.; Lan, Y. Q.; Su, Z. M. A Microporous Anionic Metal-Organic Framework for Sensing Luminescence of Lanthanide(III) Ions and Selective Absorption of Dyes by Ionic Exchange. *Chem. - Eur. J.* **2014**, *20*, 5625–5630.
- (8) An, J.; Geib, S. J.; Rosi, N. L. Cation-Triggered Drug Release from a Porous Zinc-Adeninate Metal-Organic Framework. *J. Am. Chem. Soc.* **2009**, *131*, 8376–8377.
- (9) An, J.; Shade, C. M.; Chengelis-Czegán, D. A.; Petoud, S.; Rosi, N. L. Zinc-Adeninate Metal-Organic Framework for Aqueous Encapsulation and Sensitization of Near-infrared and Visible Emitting Lanthanide Cations. *J. Am. Chem. Soc.* **2011**, *133*, 1220–1223.
- (10) Zhang, S. R.; Li, J.; Du, D. Y.; Qin, J. S.; Li, S. L.; He, W. W.; Su, Z. M.; Lan, Y. Q. A Multifunctional Microporous Anionic Metal-

Organic Framework for Column-Chromatographic Dye Separation and Selective Detection and Adsorption of Cr^{3+} . *J. Mater. Chem. A* **2015**, *3*, 23426–23434.

(11) Xie, W.; He, W. W.; Li, S. L.; Shao, K. Z.; Su, Z. M.; Lan, Y. Q. An Anionic Interpenetrated Zeolite-Like Metal-Organic Framework Composite As a Tunable Dual-Emission Luminescent Switch for Detecting Volatile Organic Molecules. *Chem. - Eur. J.* **2016**, *22*, 17298–17304.

(12) Wang, D.; Zhang, J.; Li, G.; Yuan, J.; Li, J.; Huo, Q.; Liu, Y. Mesoporous Hexanuclear Copper Cluster-Based Metal-Organic Framework with Highly Selective Adsorption of Gas and Organic Dye Molecules. *ACS Appl. Mater. Interfaces* **2018**, *10*, 31233–31239.

(13) Wang, Z.; Zhang, J. H.; Jiang, J. J.; Wang, H. P.; Wei, Z. W.; Zhu, X.; Pan, M.; Su, C. Y. A Stable Metal Cluster-Metalloporphyrin MOF With High Capacity for Cationic Dye Removal. *J. Mater. Chem. A* **2018**, *6*, 17698–17705.

(14) Tan, Y. C.; Zeng, H. C. Defect Creation in HKUST-1 via Molecular Imprinting: Attaining Anionic Framework Property and Mesoporosity for Cation Exchange Applications. *Adv. Funct. Mater.* **2017**, *27*, 1703765.

(15) He, Y. C.; Yang, J.; Kan, W. Q.; Zhang, H. M.; Liu, Y. Y.; Ma, J. F. A New Microporous Anionic Metal-Organic Framework as a Platform for Highly Selective Adsorption and Separation of Organic Dyes. *J. Mater. Chem. A* **2015**, *3*, 1675–1681.

(16) Johnson, J. A.; Luo, J.; Zhang, X.; Chen, Y. S.; Morton, M. D.; Echeverría, E.; Torres, F. E.; Zhang, J. Porphyrin-Metalation-Mediated Tuning of Photoredox Catalytic Properties in Metal-Organic Frameworks. *ACS Catal.* **2015**, *5*, 5283–5291.

(17) Zhang, T.; Manna, K.; Lin, W. Metal-Organic Frameworks Stabilize Solution-Inaccessible Cobalt Catalysts for Highly Efficient Broad-Scope Organic Transformations. *J. Am. Chem. Soc.* **2016**, *138*, 3241–3249.

(18) Xiao, J.; Liu, J.; Gao, X.; Ji, G.; Wang, D.; Liu, Z. A multi-chemosensor based on Zn-MOF: Ratio-Dependent Color Transition Detection of Hg (II) and Highly Sensitive Sensor of Cr (VI). *Sens. Actuators, B* **2018**, *269*, 164–172.

(19) Lv, R.; Wang, J.; Zhang, Y.; Li, H.; Yang, L.; Liao, S.; Gu, W.; Liu, X. An Amino-Decorated Dual-Functional Metal-Organic Framework for Highly Selective Sensing of Cr(III) and Cr(VI) Ions and Detection of Nitroaromatic Explosives. *J. Mater. Chem. A* **2016**, *4*, 15494–15500.

(20) Hu, J. S.; Dong, S. J.; Wu, K.; Zhang, X. L.; Jiang, J.; Yuan, J.; Zheng, M. D. An Ultrastable Magnesium-Organic Framework As Multi-Responsive Luminescent Sensor for Detecting Trinitrotoluene and Metal Ions with High Selectivity and Sensitivity. *Sens. Actuators, B* **2019**, *283*, 255–261.

(21) Razavi, S. A. A.; Morsali, A. Metal Ion Detection Using Luminescent-MOFs: Principles, Strategies and Roadmap. *Coord. Chem. Rev.* **2020**, *415*, 213299.

(22) Chen, W. M.; Meng, X. L.; Zhuang, G. L.; Wang, Z.; Kurmoo, M.; Zhao, Q. Q.; Wang, X. P.; Shan, B.; Tung, C. H.; Sun, D. A Superior Fluorescent Sensor for Al^{3+} and UO_2^{2+} Based on a Co(II) Metal-Organic Framework with Exposed Pyrimidyl Lewis Base Sites. *J. Mater. Chem. A* **2017**, *5*, 13079–13085.

(23) Li, Q.; Wu, X.; Huang, X.; Deng, Y.; Chen, N.; Jiang, D.; Zhao, L.; Lin, Z.; Zhao, Y. Tailoring the Fluorescence of AIE-Active Metal-Organic Frameworks for Aqueous Sensing of Metal Ions. *ACS Appl. Mater. Interfaces* **2018**, *10*, 3801–3809.

(24) Hu, Z.; Deibert, B. J.; Li, J. Luminescent Metal-Organic Frameworks for Chemical Sensing and Explosive Detection. *Chem. Soc. Rev.* **2014**, *43*, 5815–5840.

(25) Kreno, L. E.; Leong, K.; Farha, O. K.; Allendorf, M.; Van Dwyne, R. P.; Hupp, J. T. Metal-Organic Framework Materials as Chemical Sensors. *Chem. Rev.* **2012**, *112*, 1105–1125.

(26) Liu, C.; Yan, B. A Novel Photofunctional Hybrid Material of Pyrene Functionalized Metal-Organic Framework with Conformation Change for Fluorescence Sensing of Cu^{2+} . *Sens. Actuators, B* **2016**, *235*, 541–546.

(27) Hao, J. N.; Yan, B. Amino-Decorated Lanthanide(III) Organic Extended Frameworks for Multi-Color Luminescence and Fluorescence Sensing. *J. Mater. Chem. C* **2014**, *2*, 6758–6764.

(28) Wang, H.; Qin, J.; Huang, C.; Han, Y.; Xu, W.; Hou, H. Mono/bimetallic Water-Stable Lanthanide Coordination Polymers as Luminescent Probes for Detecting Cations, Anions and Organic Solvent Molecules. *Dalton T.* **2016**, *45*, 12710–12716.

(29) Chen, Y. Z.; Jiang, H. L. Porphyrinic Metal-Organic Framework Catalyzed Heck-Reaction: Fluorescence “Turn-On” Sensing of Cu(II) Ion. *Chem. Mater.* **2016**, *28*, 6698–6704.

(30) Feng, X.; Feng, Y.; Guo, N.; Sun, Y.; Zhang, T.; Ma, L.; Wang, L. Series d-f Heteronuclear Metal-Organic Frameworks: Color Tunability and Luminescent Probe with Switchable Properties. *Inorg. Chem.* **2017**, *56*, 1713–1721.

(31) Zhang, Y. B.; Furukawa, H.; Ko, N.; Nie, W.; Park, H. J.; Okajima, S.; Cordova, K. E.; Deng, H.; Kim, J.; Yaghi, O. M. Introduction of Functionality, Selection of Topology, and Enhancement of Gas Adsorption in Multivariate Metal-Organic Framework-177. *J. Am. Chem. Soc.* **2015**, *137*, 2641–2650.

(32) Lan, Y. Q.; Li, S. L.; Jiang, H. L.; Xu, Q. Tailor-Made Metal-Organic Frameworks from Functionalized Molecular Building Blocks and Length-Adjustable Organic Linkers by Stepwise Synthesis. *Chem. - Eur. J.* **2012**, *18*, 8076–8083.

(33) Mao, C.; Kudla, R. A.; Zuo, F.; Zhao, X.; Mueller, L. J.; Bu, X.; Feng, P. Anion Stripping as a General Method to Create Cationic Porous Framework with Mobile Anions. *J. Am. Chem. Soc.* **2014**, *136*, 7579–7582.

(34) Zhao, X.; Mao, C.; Luong, K. T.; Lin, Q.; Zhai, Q. G.; Feng, P.; Bu, X. Framework Cationization by Preemptive Coordination of Open Metal Sites for Anion-Exchange Encapsulation of Nucleotides and Coenzymes. *Angew. Chem., Int. Ed.* **2016**, *55*, 2768–2772.

(35) Zhao, X.; Bu, X.; Wu, T.; Zheng, S. T.; Wang, L.; Feng, P. Selective Anion Exchange with Nanogated Isoreticular Positive Metal-Organic Frameworks. *Nat. Commun.* **2013**, *4*, 2344.

(36) Lin, Z. J.; Huang, Y. B.; Liu, T. F.; Li, X. Y.; Cao, R. Construction of a Polyhedral Metal-Organic Framework via a Flexible Octacarboxylate Ligand for Gas Adsorption and Separation. *Inorg. Chem.* **2013**, *52*, 3127–3132.

(37) Huang, P.; Chen, C.; Wu, M.; Jiang, F.; Hong, M. An Indium-Organic Framework for the Efficient Storage of Light Hydrocarbons and Selective Removal of Organic Dyes. *Dalton T.* **2019**, *48*, 5527–5533.

(38) Luo, Y. H.; Xie, A. D.; Chen, W. C.; Shen, D.; Zhang, D. E.; Tong, Z. W.; Lee, C. S. Multifunctional Anionic Indium-Organic Frameworks for Organic Dye Separation, White-Light Emission and Dual-Emitting Fe^{3+} Sensing. *J. Mater. Chem. C* **2019**, *7*, 14897–14903.

(39) Spek, A. Structure validation in chemical crystallography. *Acta Crystallogr., Sect. D: Biol. Crystallogr.* **2009**, *65*, 148–155.

(40) Liu, X.; Hao, C.; Li, J.; Wang, Y.; Hou, Y.; Li, X.; Zhao, L.; Zhu, H.; Guo, W. An Anionic Metal-Organic Framework: Metathesis of Zinc(II) With Copper(II) for Efficient C3/C2 Hydrocarbon and Organic Dye Separation. *Inorg. Chem. Front.* **2018**, *5*, 2898–2905.

(41) Wei, Z.; Gu, Z. Y.; Arvapally, R. K.; Chen, Y. P.; McDougald, R. N.; Ivy, J. F.; Yakovenko, A. A.; Feng, D.; Omary, M. A.; Zhou, H. C. Rigidifying Fluorescent Linkers by Metal-Organic Framework Formation for Fluorescence Blue Shift and Quantum Yield Enhancement. *J. Am. Chem. Soc.* **2014**, *136*, 8269–8276.

(42) Zhang, H. M.; Yang, J.; Liu, Y. Y.; Kang, D. W.; Ma, J. F. A Family of Coordination Polymers Assembled With a Flexible Hexacarboxylate Ligand and Auxiliary N-donor Ligands: Syntheses, Structures, and Physical Properties. *CrystEngComm* **2015**, *17*, 3181–3196.

(43) Wang, H. N.; Meng, X.; Qin, C.; Wang, X. L.; Yang, G. S.; Su, Z. M. A Series of Pillar-Layer Metal-Organic Frameworks Based on 5-Aminoisophthalic Acid and 4,4'-Bipyridine. *Dalton T.* **2012**, *41*, 1047–1053.

(44) Xiang, Z.; Fang, C.; Leng, S.; Cao, D. An Amino Group Functionalized Metal-Organic Framework As a Luminescent Probe

for Highly Selective Sensing of Fe^{3+} Ions. *J. Mater. Chem. A* **2014**, *2*, 7662–7665.

(45) Wiwasaku, T.; Othong, J.; Boonmak, J.; Ervithayasuporn, V.; Youngme, S. Sonochemical Synthesis of Microscale $\text{Zn}(\text{II})$ -MOF With Dual Lewis Basic Sites for Fluorescent Turn-On Detection of Al^{3+} and Methanol With Low Detection Limits. *Dalton T.* **2020**, *49*, 10240–10249.

(46) Ye, J.; Wang, X.; Bogale, R. F.; Zhao, L. M.; Cheng, H.; Gong, W. T.; Zhao, J. Z.; Ning, G. L. A Fluorescent Zinc-Pamoate Coordination Polymer for Highly Selective Sensing of 2,4,6-Trinitrophenol and Cu^{2+} Ion. *Sens. Actuators, B* **2015**, *210*, 566–573.

(47) Li, P. C.; Zhang, L.; Yang, M.; Zhang, K. L. A Novel Luminescent 1D→2D Polyrotaxane $\text{Zn}(\text{II})$ -Organic Framework Showing Dual Responsive Fluorescence Sensing for Fe^{3+} Cation and $\text{Cr}(\text{VI})$ Anions in Aqueous Medium. *J. Lumin.* **2019**, *207*, 351–360.

(48) Guo, X. Y.; Zhao, F.; Liu, J. J.; Liu, Z. L.; Wang, Y. Q. An Ultrastable Zinc(II)-Organic Framework as a Recyclable Multi-Responsive Luminescent Sensor for $\text{Cr}(\text{III})$, $\text{Cr}(\text{VI})$ and 4-Nitrophenol in the Aqueous Phase With High Selectivity and Sensitivity. *J. Mater. Chem. A* **2017**, *5*, 20035–20043.

(49) Yang, Y. J.; Wang, M. J.; Zhang, K. L. A Novel Photoluminescent $\text{Cd}(\text{II})$ -Organic Framework Exhibiting Rapid and Efficient Multi-Responsive Fluorescence Sensing for Trace Amounts of Fe^{3+} Ions and Some NACs, Especially for 4-Nitroaniline and 2-Methyl-4-nitroaniline. *J. Mater. Chem. C* **2016**, *4*, 11404–11418.